Computer-simulation studies of kinetic gelation

Y. Liu
Program in Scientific Computing, University of Southern Mississippi, Hattiesburg, Mississippi 39406-5046

R. B. Pandey
Program in Scientific Computing and Department of Physics and Astronomy, University of Southern Mississippi, Hattiesburg, Mississippi 39406-5046

(Received 17 July 1996; revised manuscript received 7 November 1996)

Computer simulations are performed to study kinetic gelation on a simple cubic lattice. Two models are considered: (1) irreversible gelation in which the monomers and microgels attempt to react with their neighboring particles with a certain probability (p_b) and (2) reversible gelation in which the bonds are broken with a certain probability (p_r). The growth of the extent of reaction (i.e., the concentration of the bonds grown), volume fraction of the gel, weight average degree of polymerization, and the correlation length are studied as a function of p_b and p_r. We observe that (i) the concentration of bonds grows nonlinearly with time. (ii) The critical gel time (t_c) increases nonlinearly on increasing the degree of reversibility, p_r, while the critical concentration (p_c) at the gel point is insensitive to p_b and p_r. (iii) For large p_r, our data suggest that the sol-to-gel transition may be nonuniversal. [S0163-1829(97)05513-6]

I. INTRODUCTION

Modeling kinetic gelation has been the subject of continued interest.[1–6] Kinetic gelation involves stochastic growth processes in which ramified networks of chemical species evolve due to a variety of physical and chemical processes, leading to entanglement and cross-linking of various order. Such kinetic processes lead to a diverse range of form, growth, and decay of the gel network and microgel particles, with a wide distribution of loop sizes, dangling ends, branching, multiplicity in bonding, etc. Some of the physical properties of the gel and microgels, such as weight-average degree of polymerization (WADP), volume fraction, distribution of pores, and branching, can be modified by altering the process and varying the parameters. Even with the existing well-developed gelation methods, it is rather difficult to predict the stochastic nature of porous gels. It is therefore important to develop and investigate the behavior of simplified models.

The classical approach of percolation on the Cayley tree due to Flory[1] and Stockmayer[2] is regarded as the starting point in the theory of irreversible kinetic gelation. Although such mean-field models have drawbacks, for the lack of excluded volume, steric hindrance, and closed loops, they allow derivation of closed-form expressions for physical quantities such as the volume fraction and WADP and have helped elucidate features of the sol-to-gel transition. Enormous efforts have been made to develop improved models. For example, the percolation on three-dimensional lattices proposed by de Gennes and Stauffer[7–9] takes into account cyclization and branches, and can describe the sol-to-gel transition with more accurate exponents. However, such percolation models can also be criticized due to a lack of realistic reaction kinetics and multiplicity in bond formation.

Kinetic gelation begins in the sol (solution) phase. Large macromolecules (microgel particles) form, and the viscosity increases, as the reaction proceeds. At a certain reaction time, an ''infinite'' macromolecule, an incipient infinite network appears, the viscosity of the system diverges (as does the correlation length and WADP), and the elastic nature of the gel sets in. The extent of reaction (or time) at which the onset of gelation occurs is defined as the critical gel point, above which an infinite network (gel) coexists with sol and microgel particles. The singularities at the gel point are usually characterized by critical exponents accessible from scattering measurements. Many experiments have been performed to estimate these critical exponents in different gelation systems.[10–23] It is believed that in polymer systems, there exists a crossover between the classical theory of Flory and Stockmayer and three-dimensional percolation theory.

Extensive computer simulation studies of realistic models for irreversible kinetic gelation[3,24–27] have been performed. However, most of these studies have been restricted to static growth in the sense that the chemical constituents were immobile during the course of the reaction except for the active centers (i.e., the free radicals) and the solvent. The mobility of the solvent, monomers, and microgel particles has been considered in recent computer simulation studies.[28–30] For example, Bowman and Peppas examined free-radical polymerization[28] of tetrafunctional monomers in which a monomer can occupy multiple sites. Chiu and Lee[30] considered the mobility of the monomers and polymer molecules, and studied the polymer size distribution and the reaction rates. These studies are, however, limited to small sample sizes. Furthermore, while these investigations emphasize the reaction kinetics such as the conversion rate, the sol-to-gel transition is not studied in detail. In one of our previous simulations, we studied[31] the sol-to-gel transition with a low concentration of bifunctional and tetrafunctional monomers by a computer simulation model in three dimensions in which monomers and microgels are mobile. We assumed that the hopping rate of these particles is inversely proportional to their mass and that bonds are formed with a certain probability after a certain number of hopping attempts. One

of the major results of this study was that the gel point depends strongly on particle mobility.

Some attempts have also been made to take into account the effects of diffusion of polymer units in off-lattice models.[32,33] Leung and Eichinger[32] developed a computer simulation model to study the critical behavior of gelation for various types of nonlinear polymers, focusing on the effect of intramolecular reactions. The growth of the molecules proceeded by joining available neighboring reactive groups within a reactive radius. Gupta *et al.*[33] developed a similar model to investigate diffusional effects. They found that, with decreasing reactive radius, the critical exponents show a crossover from the infinite diffusion mean-field model to standard percolation theory.[34]

It is worth mentioning that there have been several studies of aggregation models in which the mobility of the clusters was considered[3–6,35–37] which suggests that the ramification of the aggregate clusters is enhanced and the fractal dimensionality is reduced due to mobility. However, unlike in kinetic gelation models, functionality of the particles is not restricted. In any case, most of these studies emphasize the fractal dimensionality rather than the sol-to-gel transition. An alternate approach to study kinetic gelation, in which the mobility of the particles and clusters is included, is the so-called continuum approach.[38,39] Here, one studies the behavior of Smoluchowski-type differential equations for the growth and decay of the clusters. For certain kernels, i.e., rate constants for cluster aggregation and decay, it is rather easy to study the growth of the cluster size and to estimate the sol-to-gel critical exponents. However, in more general situations (i.e., for spatiotemporal-dependent rate constants), such equations become intractable. Furthermore, it is not clear if the nonlinearity of the medium (i.e., spatial inhomogeneities) and the steric hindrance can be taken into account appropriately in such approaches.

Most of these investigations were restricted to irreversible kinetic gelation. In contrast, gelation processes in the laboratory possess some degree of reversibility.[40–45] To our knowledge, there are only a few systematic computer simulation studies[46,47] of reversible kinetic gelation. Ideally, one would like to consider all the microscopic details that govern particle mobility, formation of bonds, and their decay, but this is not feasible due to limitations on computing resources. However, we speculate that a probabilistic approach to forming bonds and to their decay would capture some of these important effects. In this paper we attempt such an investigation.

II. MODEL AND QUANTITIES OF INTEREST

We consider bifunctional and tetrafunctional monomers. A monomer is represented by a point on a discrete lattice of size $L\times L\times L$. Structural details on a scale smaller than the size of a monomer are ignored. A bifunctional monomer can react with two neighboring monomers while a tetrafunctional monomer reacts with four neighboring monomers; two neighboring monomers can be connected by only a single bond in this model. The bifunctional and tetrafunctional monomers are initially distributed randomly on a fraction C_2 and C_4 of the lattice sites, respectively. A lattice site cannot be occupied by more than one monomer. We consider a small concentration of monomers in this study by keeping C_2+C_4 fixed to 0.5 except one set with $C_2=0.2$ and $C_4=0.4$ to see the difference as indicated below. The empty sites play the role of the solvent, although no interaction is considered between a monomer and a solvent, except for the hardcore.

Monomers move in such a way that each monomer can exchange its position with one of the randomly selected solvent (i.e., empty) sites. Movement of the monomers and their reaction is implemented as follows. A randomly selected monomer/microgel particle is attempted to move in one of the six directions chosen randomly, by a unit distance (i.e., one lattice constant). If the neighboring site (sites) in this direction is (are) empty, then the monomer (particle) is moved. The attempt to move each monomer once, regardless of success, defines one Monte Carlo step (MCS), the unit for time. After hopping, each monomer attempts to react with one of their randomly selected neighboring monomers with a certain bonding probability p_b. As the reaction proceeds, clusters of monomers, i.e., the microgel particles with various shape and sizes, begin to form. The microgel particles are also mobile and the hopping rate h inversely proportional to their mass (i.e., $h=1/s$ where s is the number of monomers in a microgel particle). Note that the definition of unit time is arbitrary. Since the number of particles, i.e., the total number of unreacted monomers and microgel clusters, varies as the reaction proceeds, the unit of MCS varies accordingly. Such variable time units are frequently used in MC simulations where the number of particles varies. In our simulation, we keep track of the physical quantities at much lower time scales (i.e., at fractions of a MCS). So far the gelation is irreversible: The bonds formed between particles with probability p_b are permanent. We consider reversibility by breaking the bonds with a certain fragmentation probability (p_r).

Motivation for our choice of hopping rate $h\sim 1/s$, to describe the diffusion of a ''large'' solute in a ''small'' solvent, comes from Stokes-Einstein theory.[35] Here, the diffusion constant $D\propto R^{-1}$, where R is the radius of the large particle. Such descriptions are used for compact large objects with surface area ($\sim R^2$) much smaller than the volume ($\sim R^3$). In our case, the large solute particles are clusters which are highly ramified and seem to exhibit a fractal[2] nature. The surface area in such fractal objects is comparable to the volume; i.e., most of the cluster sites have the possibility to be in contact with the solvent particles. Thus the diffusion of a ramified fractal cluster may experience more drag than a compact object of comparable size. Therefore, we assume $h\sim 1/s$ rather than $h\sim 1/R_s$, in the spirit of the classic Stokes-Einstein theory. A further technical consideration motivated this choice. If we had to use a hopping rate that depends on R_s, then we would have to calculate R_s at each time step and this would be expensive computationally. In principle, one may try different choices for h, which may require more computing resources, but we will use $h\sim 1/s$ in this paper. The choice h governs the diffusion of particles, which affects the gel point. Thus, a different choice of h may shift our plots, but the qualitative behaviors may not change. This may be the subject of another research project.

During the simulation we calculate the evolution of various quantities described below. For constant p_b and p_r the whole simulation is repeated for a large number of indepen-

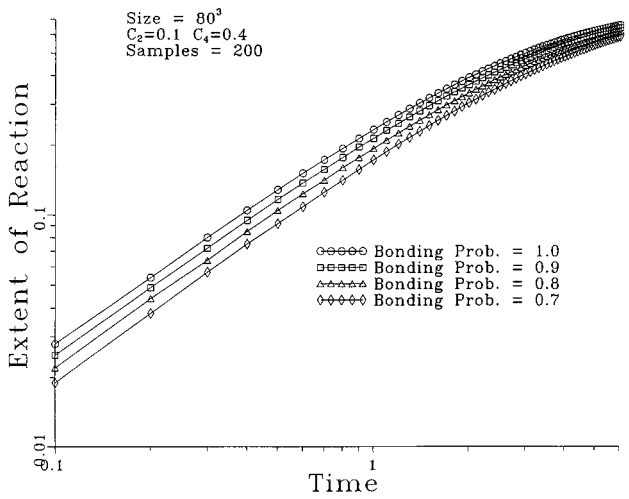

FIG. 1. Extent of reaction (p) vs time, for $p_b=1.0$, 0.9, 0.8, 0.7 on a $80\times80\times80$ site lattice. $C_2=0.1$ and $C_4=0.4$ here and in all the following figures, unless specified otherwise.

dent runs to obtain a reliable estimate of the average values of these quantities. In the initial period of polymerization, clusters are small and isolated and the whole system is in the sol phase. As the polymerization proceeds, the probability of forming larger clusters increases, and the mobility of the microgel particles decreases. The onset of gelation occurs when the incipient infinite cluster appears at the gel point, defining the critical gel time (t_c) and the critical bond concentration (p_c). Beyond the gel point, the infinite cluster coexists with the microgel particles. Although the microgel particles are still mobile, the gel network becomes immobile after the gel point. We study the sol-to-gel transition by analyzing physical quantities similar to those in percolation as described briefly next.

The extent of reaction or the concentration p of bonds at a time t is defined as the fraction of bonds formed. The volume fraction (P_G) of the gel is defined as the fraction of monomers in the infinite (gel) network, i.e.,

$$P_G=\frac{N_m}{(C_2+C_4)\times L^3}, \tag{1}$$

where N_m is the number of monomers forming the gel network. The WADP is defined as

$$S=\frac{\Sigma_s n_s s^2}{\Sigma_s s n_s}, \tag{2}$$

where s is the number of monomers and n_s is the number of clusters with s monomers per site; the infinite cluster is excluded from the summation. The correlation length ξ is defined as

$$\xi^2=\frac{2\Sigma_s(R_s{}^2 s^2 n_s)}{\Sigma_s s^2 n_s}, \tag{3}$$

where

$$R_s^2=\sum_s \frac{(r_i-r_o)^2}{s}, \tag{4}$$

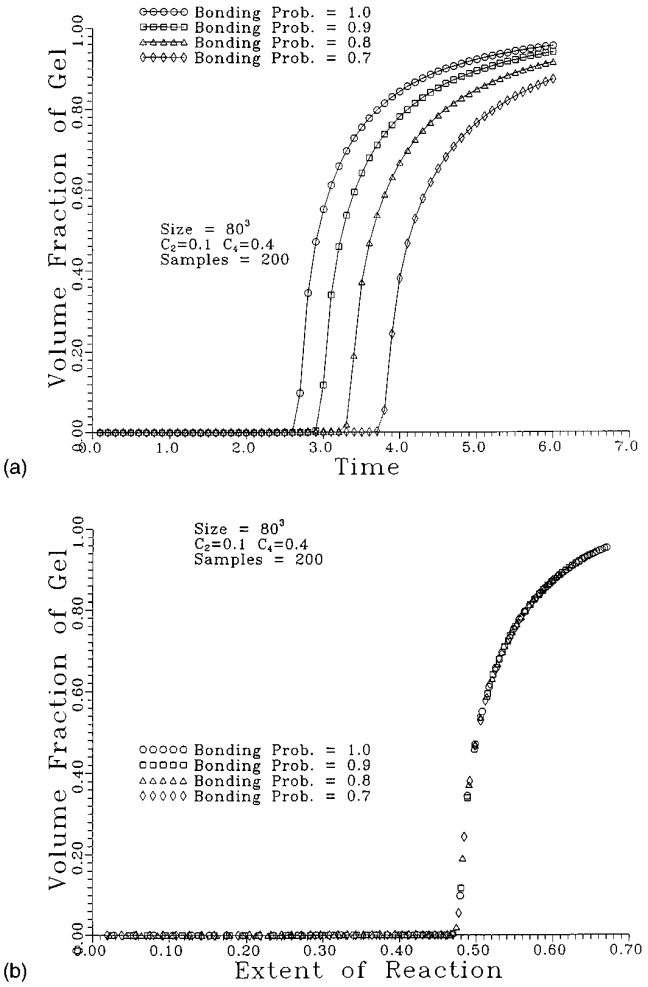

FIG. 2. Volume fraction of gel vs time (a) and vs the extent of reaction (b), for various p_b. Note that $p_c\simeq0.47$ is independent of p_b.

and

$$r_o=\frac{\Sigma_s r_i}{s}. \tag{5}$$

We have studied these quantities as a function of p. Since p depends on time, we have also studied the temporal dependence of these quantities (see the next section). Statistics are obtained from 200 independent samples for each set of parameters.

III. PROBABILISTIC IRREVERSIBLE GELATION

As we mentioned above, we consider a dilute solution of bifunctional and tetrafunctional monomers which occupy half of the lattice sites ($C_2+C_4=0.5$) in all but one case where $C_2=0.2$ and $C_4=0.4$. The particles (monomers and microgel) execute their stochastic motion with equal probability in each of the six directions. The hopping rate is, however, inversely proportional to their mass as we discussed in the previous section. After hopping, each particle (monomer or microgel) attempts to bond with one of its neighboring particles with probability p_b. The extreme value

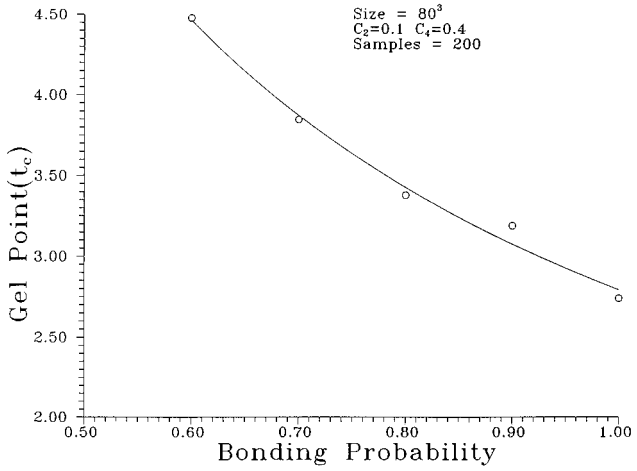

FIG. 3. Gel point t_c vs p_b.

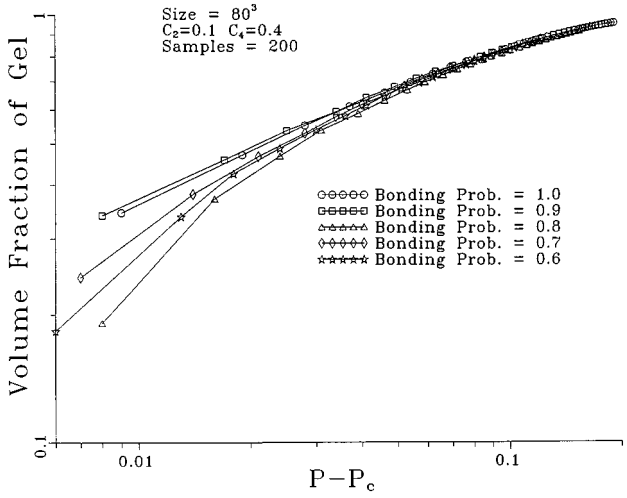

FIG. 4. Volume fraction of gel, P_G, vs $p-p_c$, for various p_b.

of $p_b=1$ leads to irreversible gelation, where the conformation of the gel is far from equilibrium. On reducing p_b, the relaxation of the gel conformation may be enhanced as the monomers and the microgel particles move around, exploring various configurations, before they permanently bond together — thus we expect that the mobility will help relaxing the gel structure. Here we focus on the effects of reducing p_b on the sol-gel transition.

Figure 1 shows the growth of the concentration of the bonds with time (in MCS). We immediately note that the fraction of bonds does not grow linearly with time. In the short-time (pre-gel) regime, however, it is linear, and can be described by a power law

$$p=At^x, \tag{6}$$

where $x\simeq 1$ for all p_b studied. The prefactor A depends on p_b, i.e., it decreases on decreasing p_b. We see a deviation from this power-law behavior in the long time (i.e., critical gel) regime. Since each monomer has unsaturated bonds initially, they succeed in forming bonds with their neighbors with probability p_b. Therefore, the rate of reaction depends only on p_b in the short time. The monomers become saturated as they bond with their neighboring molecules using all their active bonds (i.e., two for bifunctional and four for tetrafunctional monomers) as the reactions proceed in long time. Microgels become larger, resulting in their reduced mobility. Both the increased saturation and reduced mobility lead to a decay in the rate of reaction in the long-time regime. Obviously, the gelation depends on the concentration of C_2 and C_4. At sufficiently low concentrations, the system will never gel, as there can be no infinite connected network.

The variation of the volume fraction of the gel with time and extent of reaction is shown in Fig. 2, for various values of p_b. We note that the gel point t_c, the time when the incipient infinite gel network appears, increases on reducing p_b. However, the critical bond concentration p_c is not as sensitive to p_b. In fact, the data for different values of p_b collapse on the same curve for the entire range of p except near p_c. Such a difference in the variation of P_G with t and p is consistent with the nonlinear growth of p with t (i.e., the rate of reaction). Figure 3 shows the variation of t_c with p_b; it seems to show an exponential dependence. Note that below a certain value p_{bc}, a lower bound on p_b, which depends on the concentration of the solution, we may never reach the gel point.

In irreversible gelation with $p_b=1$ and in percolation models,[9] the sol-to-gel transition is described by a second-order geometrical phase transition. The decay of the gel volume fraction P_G from the post-gel regime at p_c is characterized by a critical exponent β,

$$P_G\sim(p-p_c)^\beta, \quad p>p_c. \tag{7}$$

If we assume the same power-law dependence to be valid for our probabilistic irreversible model (i.e., with $p_b<1$), then the slope of the P_G versus $(p-p_c)$ plot on a log-log scale provides an estimate of β. Figure 4 shows the P_G versus $(p-p_c)$ plot for various p_b.

For $p_b\geq 0.9$, we find $\beta\simeq 0.37$ as $p\to p_c$ and $0.008<p-p_c<0.04$. However, on reducing p_b further to 0.8 and 0.7, we see a strong deviation in the slope of $\log(P_G)$ vs $\log(p-p_c)$, as $p\to p_c$ (see Fig. 4). At lower values of p_b, even the validity of a single power law can be questioned. At large values of $(p-p_c)\geq 0.05$, i.e., far from the gel point, in

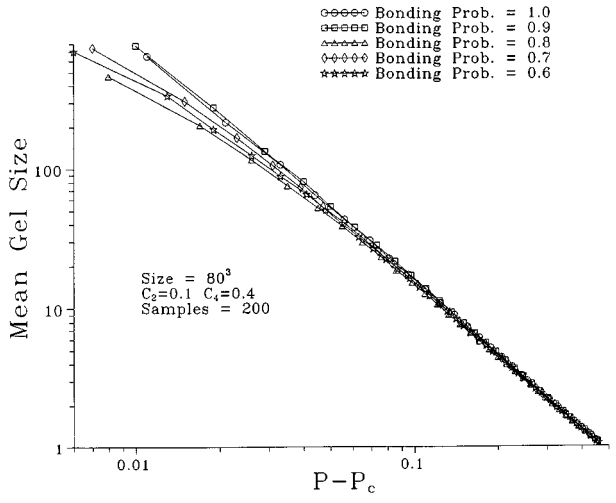

FIG. 5. Mean gel size S vs $p-p_c$, for various $p-b$.

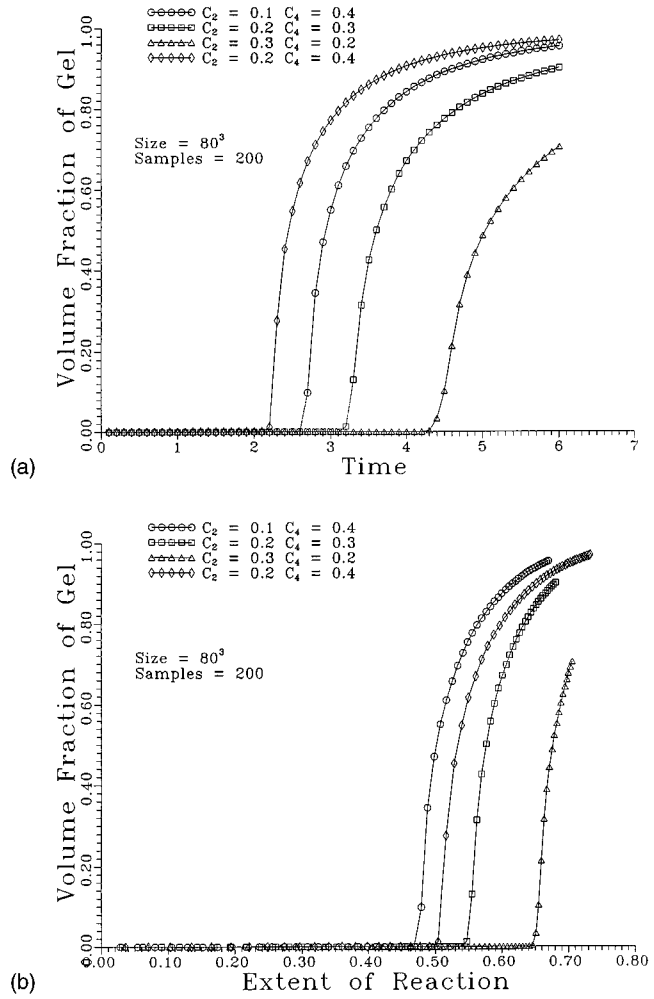

FIG. 6. (a) Volume fraction of gel vs time for various concentrations: $C_2=0.1, C_4=0.4$; $C_2=0.2, C_4=0.3$; $C_2=0.3, C_4=0.2$; $C_2=0.2, C_4=0.4$ on a $80\times80\times80$ lattice. (b) Volume fraction of gel vs the extent of reaction for various concentrations.

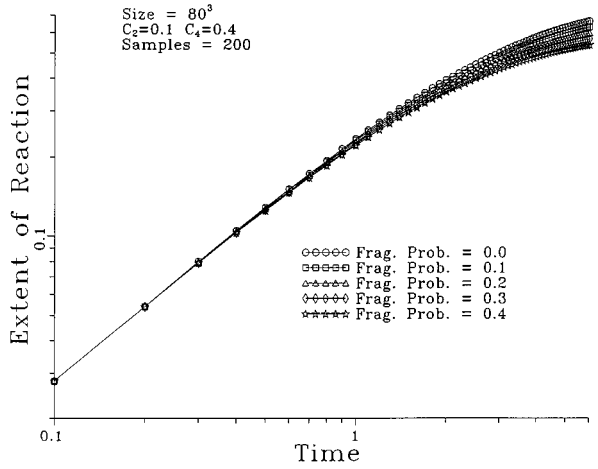

FIG. 7. Extent of reaction vs time for $p_r=0.0$, 0.1, 0.2, 0.3, 0.4, 0.5 on a $80\times80\times80$ site lattice. $C_2=0.1$ and $C_4=0.4$ here and in all the following figures, unless specified otherwise.

the post-gel regime, all the data points seem to follow the same curve. Unfortunately, these data are too far from the critical gel point to describe the sol-to-gel transition. However, these data suggest that the gel volume fraction in the post-gel regime is independent of p_b.

As we mentioned in Sec. II, the mean gel size (S) is referred to as the weight average degree of polymerization.[9] In analogy with the analysis of geometrical second-order phase transitions in static percolation and in irreversible growth ($p_b=1$), it is worth considering the power-law singularity in S at the critical gel point,

$$S\sim|p-p_c|^{-\gamma}, \tag{8}$$

where γ is the critical exponent. The $\log(S)$ versus $\log(p-p_c)$ plot is shown in Fig. 5. Since we have very few points in the critical regime for each p_b, it is difficult to find a reliable estimate of γ for all p_b. Note that with our definition of unit time step, the system gels rather fast, and so we had to consider time steps smaller than the unit step by recording physical quantities only after attempting to move a fraction of particles. Even with such a subdivision of the unit time step, we were unable to obtain sufficient statistics to evaluate γ reliably (see Fig. 5). However, at $p_b=1$ and 0.9 the data show a fairly linear fit with $\gamma\simeq1.91$. This value is consistent with that of static percolation and irreversible gelation. However, we do observe deviations at lower values of p_b (see Fig. 5).

We have also studied the variation of the correlation length ξ with time and bond concentration. Its divergence at the critical point p_c is described by

$$\xi\sim|p-p_c|^{-\nu}. \tag{9}$$

From the log-log plot of the variation of ξ with $p-p_c$, we find $\nu\simeq1$ at $p_b=1.0$ and 0.9. At lower values of p_b (0.7 and 0.8), we see deviations from Eq. (9). This is consistent with our previous observation that for lower p_b, our probabilistic irreversible gelation model may lead to a nonuniversal sol-to-gel transition.

It is interesting to explore the effects of varying the concentration of the bifunctional and tetrafunctional monomers while keeping the total concentration of the solution fixed, $C_2+C_4=0.5$. We have carried out such simulations. An additional set of data for $C_2=0.2$ and $C_4=0.4$ is also included to see the change. Plots of the gel volume fraction P_G versus time and bond concentration are presented in Fig. 6. We note that both gel points t_c and p_c decrease on decreasing C_4 and increasing C_2 at a fixed monomer concentration (0.5). Note further, by comparing the variations for the set $C_2=0.1, C_4=0.4$ and $C_2=0.2, C_4=0.3$ with that for $C_2=0.2, C_4=0.4$, that both t_c and p_c are increased by increasing C_4 from 0.3 to 0.4. On the other hand, on increasing C_2 from 0.1 to 0.2, t_c is increased but p_c is decreased somewhat. Similar behavior is also noted in the variation of other physical quantities such as S and ξ. This reflects the feature that reducing the tetrafunctional monomers reduces the formation of loops and branching, and so affects the structure and kinetics of the gel network. We are unable to comment on the effects of changing the concentrations C_2 and C_4 on the universality class of the sol-to-gel transition.

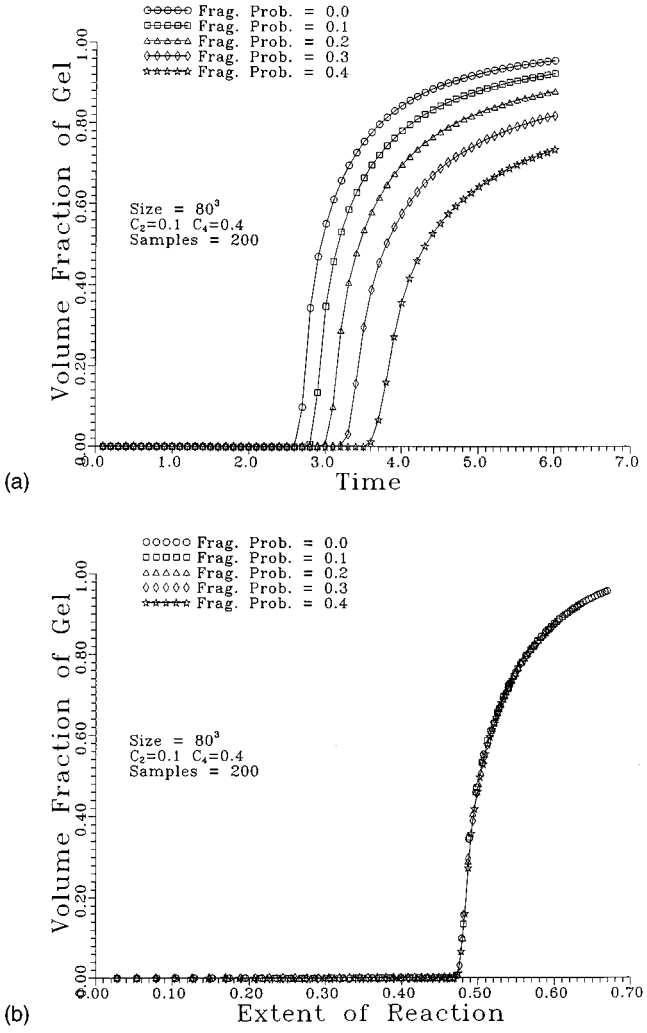

FIG. 8. Volume fraction of gel vs time (a) and vs extent of reaction (b) for various p_r.

IV. PROBABILISTIC REVERSIBLE GELATION

In this section we consider the effects of the reverse process of forming the bonds between reacting monomers. As mentioned before, the monomer and microgel particles are mobile, with the hopping rate inversely proportional to their mass. Each monomer and microgel particle attempts to bond with one of its neighboring particles, with a probability $p_b=1$, after an attempt to move. But now, each bond has a certain probability p_r of being broken, i.e., of reversing the reaction. The extreme value of this bond reversal probability, $p_r=0$, corresponds to the usual irreversible gelation. Obviously, if we increase the degree of reversibility beyond a certain value, say, p_{rc}, the system may never be able to form a stable gel network; we do not evaluate p_{rc}. In general, the magnitude of p_{rc} depends on factors such as concentration of monomers, their hopping rate, and the probability of bonding. The role of p_r in the gelation process is somewhat similar to that of temperature in thermodynamic phase transitions. The critical value of p_{rc} may correspond to the critical temperature for the magnetic phase transition. We have carried out simulations for a number of values of p_r to address the question of how the reversibility affects the sol-to-gel transition.

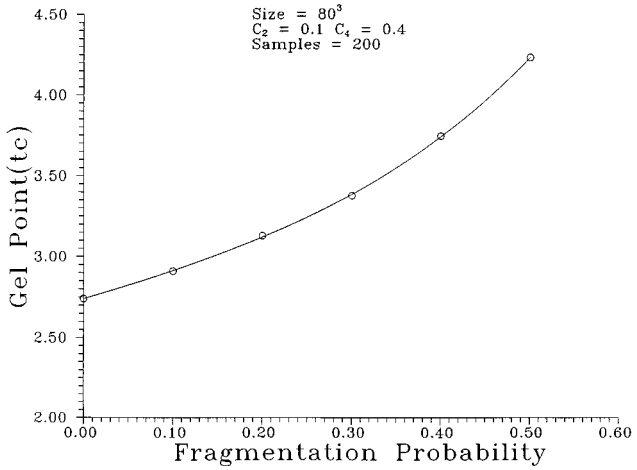

FIG. 9. Gel point t_c vs p_r.

Figure 7 shows the growth of the fraction of bonds with time for the various degrees of reversibility or fragmentation probability p_r. As in the above studies of the probabilistic irreversible gelation, the growth rate is not linear but shows a power-law growth [Eq. (6)] in the pre-gel regime; the power-law exponent $x\simeq 1$. The prefactor A is independent of p_r. Note the difference in dependence of the rate of reaction on p_r here and p_b in the preceding section (Fig. 1). In the long-time post-gel regime (i.e., at $t\sim 6$ MCS), here, the asymptotic value of the fraction of bonds, p, seems to depend systematically on p_r; it decreases on increasing p_r. Thus the rate of reaction is nonlinear with time in the critical regime ($t\sim$ 2–4 MCS).

The growth of the volume fraction of the gel with time is presented in Fig. 8(a) for various p_r. The corresponding plots for the gel volume fraction versus bond concentration are shown in Fig. 8(b). We note that the critical gelation time t_c increases, while the critical gel concentration p_c remains unchanged, on increasing p_r. The variation of t_c with p_r is presented in Fig. 9. The gel time seems to increase dramatically beyond $p_r=0.6$ where t_c diverges and the formation of a stable gel network becomes less probable. In analogy with the magnetic phase transition, we conjecture that beyond a

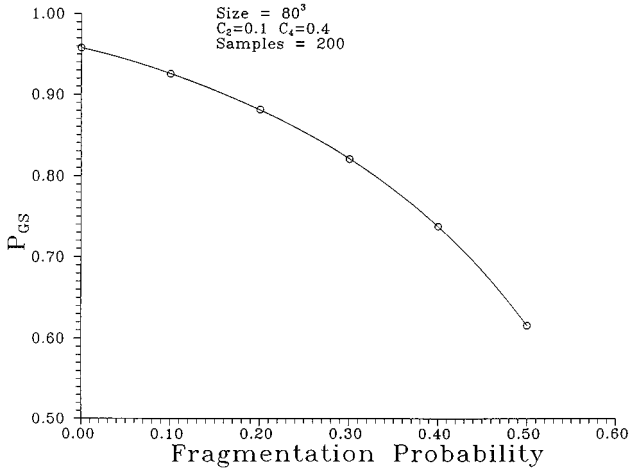

FIG. 10. Volume fraction of gel at saturation, P_{GS}, vs p_r.

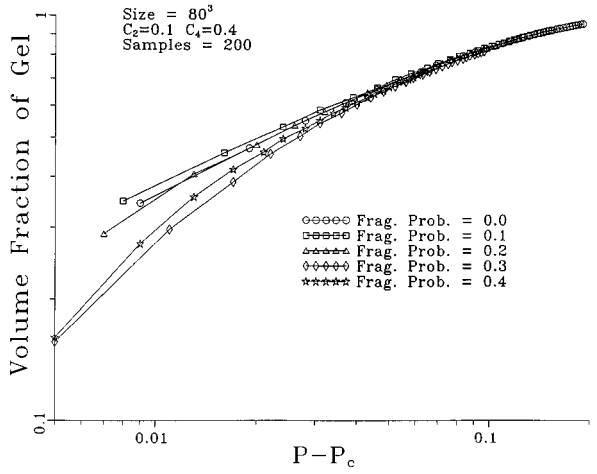

FIG. 11. Volume fraction of gel vs $p-p_c$, for various p_r.

critical value of $p_{rc}(>0.6)$ the system will never gel.

We further note from Fig. 8 that the volume fraction of the gel network seems to saturate to a certain value P_{GS} in the long-time regime. The last data points in Fig. 8(a) are not the ''true saturation'' value ($P_{G\infty}$) of P_G since the simulations are terminated before the reactions complete. This saturation value (P_{GS}) depends on p_r. From Fig. 10, it appears that P_{GS} decreases nonlinearly with p_r.

As before, we can estimate β from the $\log P_G$ versus $\log(p-p_c)$ plot (Fig. 11). We find that, as $p\rightarrow p_c$, the value of β increases on increasing p_r, from $\beta\simeq 0.37$ at $p_r=0.0$ and 0.1, to $\beta\simeq 0.5$ at $p_r=0.5$. Note that even though these estimates are crude, a systematic deviation in β is clear on increasing p_r. Thus the sol-to-gel transition seems nonuniversal for our probabilistic reversible gelation.

Variations of the mean gel size S with time and bond concentration are consistent with the data for the volume fraction of the gel, in that the critical gel time (t_c) increases on increasing p_r. From the behavior of S versus $|p-p_c|$ plot (Fig. 12), we find that γ decreases on increasing p_r; this trend supports our conjecture that the the sol-to-gel transition depends on p_r and is nonuniversal. Analogous studies have also been carried out to analyze ξ (Fig. 13). Estimates for the corresponding exponents are summarized in Table I. Attempts have also been made to evaluate the exponent $\tau(n_s(p_c)\sim s^{-\tau}$ which does not seem to be as sensitive to the degree of reversibility (see Table I). Note that, for $p_r=0$, i.e., when the gelation is irreversible, the magnitude of these exponents is close to their percolation values.

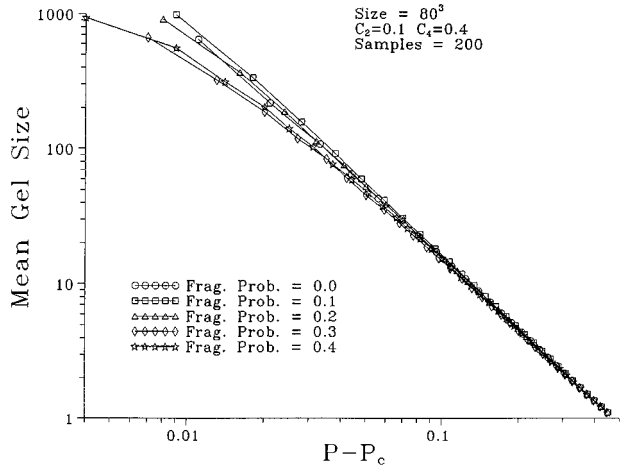

FIG. 12. Mean gel size vs $p-p_c$, for various p_r.

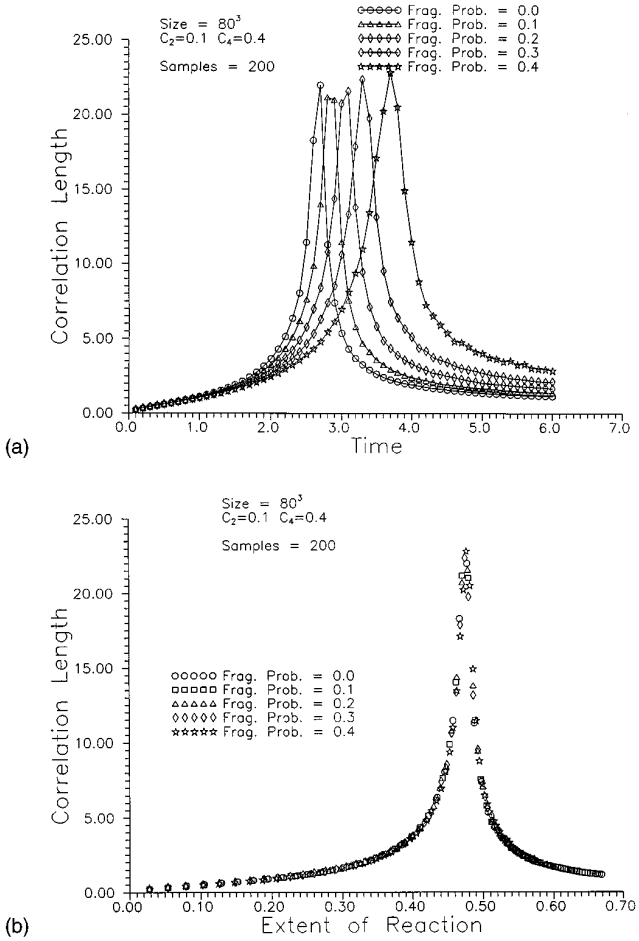

FIG. 13. Correlation length vs time (a) and vs extent of reaction (b), for various p_r.

In order to check the effects of the finite lattice size on the sol-to-gel transition, we have carried out simulations with various lattices (60^3–90^3), at $p_r = 0.4$. The variation of P_G and S with time and extent of reaction is presented in Figs. 14 and 15. We see that, despite small quantitative dif-

TABLE I. Critical exponents for the sol-to-gel transition for various degrees of reversibility (or fragmentation probability) p_r. The statistical error in the estimate of these exponents is around ± 0.10.

p_r	β	γ	ν	τ
0.0	0.37	1.91	0.95	2.16
0.1	0.37	1.82	0.98	2.17
0.2	0.39	1.88	0.90	2.17
0.3	0.57	1.66	0.98	2.25
0.4	0.58	1.74	0.99	2.24
0.5	0.65	1.54	0.75	2.31

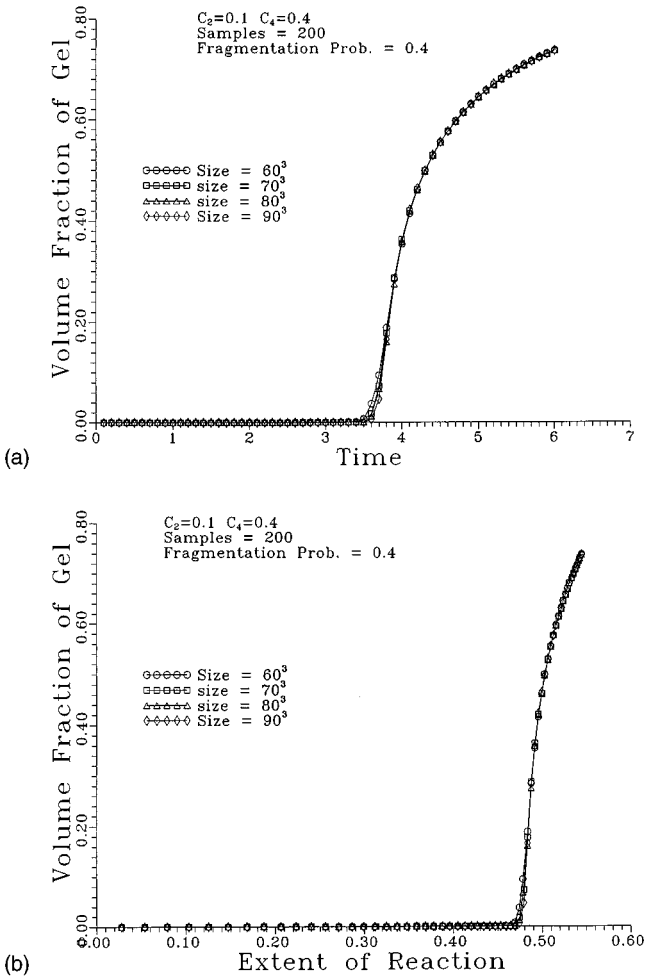

FIG. 14. (a) Volume fraction of gel vs time on lattices of various sizes: $60\times60\times60$, $70\times70\times70$, $80\times80\times80$, $90\times90\times90$, for $p_r=0.4$. $C_2=0.1$ and $C_4=0.4$ here and in all the following figures, unless specified otherwise. (b) Volume fraction of gel vs extent of reaction on lattices of various sizes.

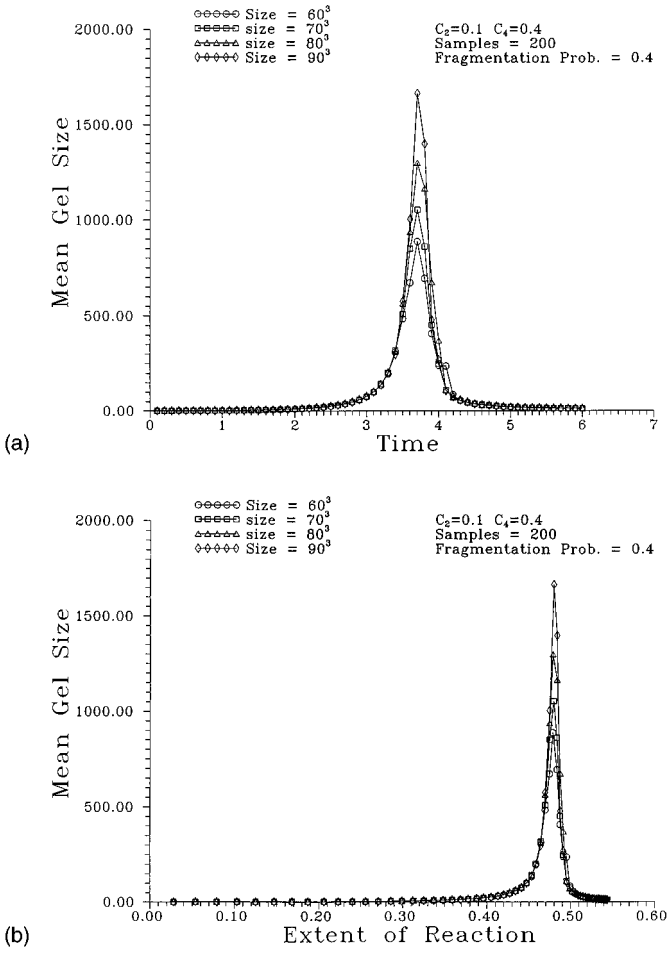

FIG. 15. Mean gel size vs time (a) and vs extent of reaction (b), on lattices of various sizes.

ferences for different lattice sizes, the qualitative behavior of these quantities remains the same; the gel point remains unchanged. Thus, we do not have severe finite-size effects that change our qualitative observations.

V. ONSET OF NONDIFFUSIVE BEHAVIOR

In the study of the sol-to-gel transition, one of the important features that distinguishes the sol phase from the gel phase is the change in the viscoelastic properties. In the sol phase where each particle is mobile, the system exhibits viscous behavior typical of liquids, while in gel phase the onset of elastic behavior of the gel network sets in.[1] One may verify this crossover behavior by analyzing the variation of the root-mean-square (rms) displacement of particles with time. We note that the number and size of particles (monomers and microgels) vary during the course of the reaction process. Thus, it is rather difficult to keep track of the temporal variation of the rms displacement of the particles of each size. However, we use a simple approach in which we evaluate the average rms displacement, calculated at equal intervals of time, and then averaged over the number of particles during these intervals. Plots of the rms displacement versus time for the probabilistic irreversible ($p_r=0$) and reversible ($p_b=1$) kinetic gelation are presented in Figs. 16 and 17. We see that the rms displacement increases rather fast in the initial stage (i.e., pre-gel regime, $t\leqslant 2$ MCS) followed by a considerable slowdown; the data in the long-time (post-gel) regime show signs of slow saturation. Note that even in the late stage of kinetic gelation some macro-

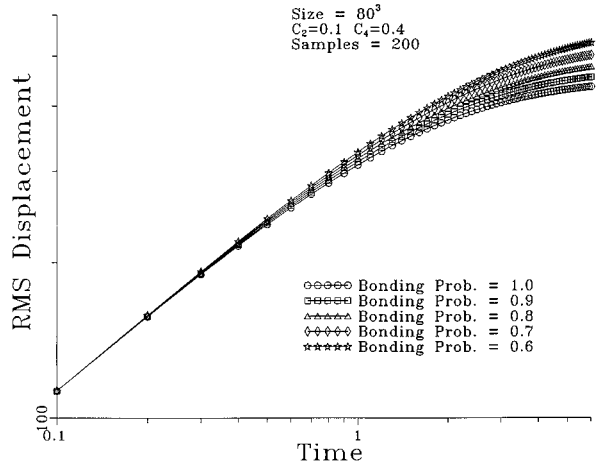

FIG. 16. rms displacement vs time for various p_b (and $p_r=0$).

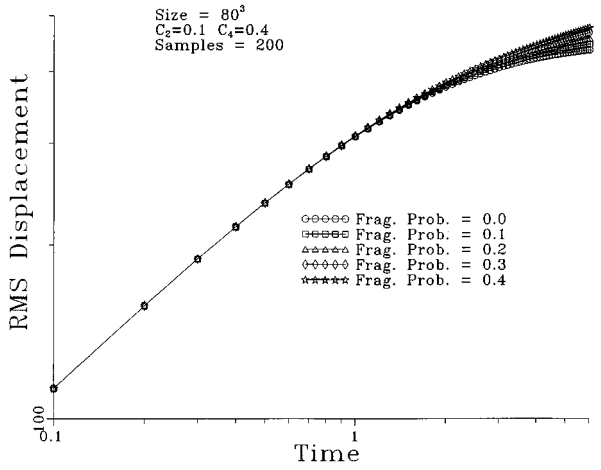

FIG. 17. rms displacement vs time for various p_r (and $p_b=1$).

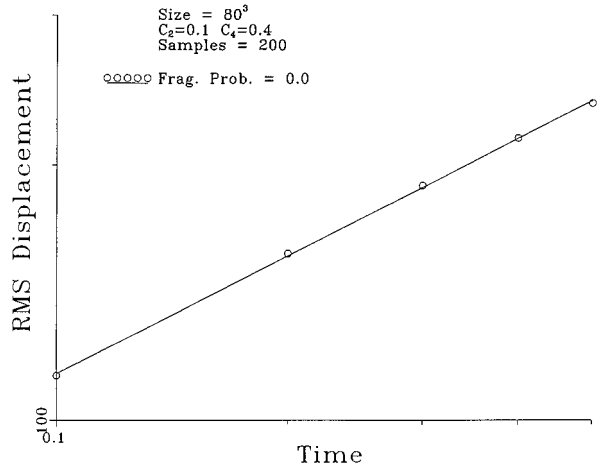

FIG. 18. rms displacement vs time in the pre-gel regime.

molecules are still mobile, and this contributes to the increase in the rms displacements, with extremely slow rates.

A close examination of these data on a log-log scale reveals the nature of the average transport behavior of the particles. The data for times up to 1 MCS (for nearly one decade, 0.1–1 MCS) show a very good power-law dependence in which the rms displacement R exhibits standard diffusive behavior, $R^2=6Dt$ (see Fig. 18). At $t\geqslant 1$, nonlinear behavior appears in the critical regime ($t\sim$ 2–4 MCS), before it reaches a quasi-steady-state limit in the late stage of the post-gel regime. In the post-gel regime, the infinite gel network is immobile, and the rate of increase of the average rms displacement with time is due to the mobility of finite clusters.

VI. SUMMARY AND CONCLUSION

A computer simulation model is presented to study the effects of athermal equilibration of the sol-to-gel transition in a step reaction kinetic gelation process in a dilute system. Two probabilistic processes are considered: reversible and irreversible growth. Particles (monomers and microgels) are mobile with hopping rate inversely proportional to their mass. Each hopping event is followed by an attempt to form a bond with the neighboring particles. In stochastic irreversible gelation bonds form with probability p_b; once a bond is formed, it is irreversible throughout the gelation. In the probabilistic reversible gelation, a bond can be broken with probability p_r. The gel grows far from equilibrium at $p_b=1$ and $p_r=0$, and there is no gelation at $p_b=0$ and $p_r=1$. The effects of athermal equilibration on the kinetics of gelation are explored by reducing p_b from 1 and increasing p_r above zero.

In the extreme limit of $p_b=1$, $p_r=0$, the critical exponents for the sol-to-gel transition remain nearly the same as those of percolation or static irreversible kinetic gelation.[27] The estimates of these exponents are consistent with theoretical as well as with experimental values.[10,16] However, on varying both the probability of bonding (p_b) and the degree of reversibility (p_r), we observe strong deviations from power-law behavior [Eqs. (8) and (9)]. Thus we conjecture that the sol-to-gel transition is nonuniversal for this model as it depends on p_r and p_b.

ACKNOWLEDGMENTS

This work was supported in part by a Cray Research grant and a NSF-EPSCoR grant. The computer simulations were performed on Cray YMP at the Mississippi Center for Supercomputing Research, and several work stations at the University of Southern Mississippi. We thank Rob Lescanec and Ken Mauritz for useful discussions.

[1] P. J. Flory, J. Am. Chem. Soc. **63**, 3083 (1941); **63**, 3091 (1941); **63**, 3096 (1941); *Principles of Polymer Chemistry* (Cornell University Press, Ithaca, 1953).

[2] W. H. Stockmayer, J. Chem. Phys. **11**, 45 (1943); **12**, 125 (1944).

[3] *Kinetics of Aggregation and Gelation*, edited by F. Family and D. P. Landau (North-Holland, Amsterdam, 1984).

[4] *Random Fluctuations and Pattern Growth*, edited by H. E. Stanley and N. Ostrowsky (Kluwer Academic, Norwell, Massachusetts, 1988).

[5] M. Kolb, in *Fractals in Physics*, edited by L. Pietronero and E. Tosatti (Elsevier, New York, 1986).

[6] M. Klob and H. J. Herrmann, J. Phys. A **18**, L435 (1985).

[7] P. G. de Gennes, J. Phys. France Lett. **37**, L1 (1976).

[8] D. Stauffer, J. Chem. Soc. Faraday Trans. II **72**, 1354 (1976).

[9] D. Stauffer, A. Coniglio, and M. Adam, Adv. Polym. Sci. **41**, 103 (1982).

[10] M. Daoud, F. Family, and G. Jannink, J. Phys. Lett. (Paris) **45**, L199 (1984).

[11] J. E. Martin, J. Wilcoxon, and D. Adolf, Phys. Rev. A **36**, 1803 (1987).

[12] M. Adam, M. Delsanti, J. P. Munch, and D. Durand, J. Phys. (France) **48**, 1809 (1987).

[13] E. V. Patton, J. A. Wesson, M. Rubinstein, J. C. Wilson, and L. E. Oppenheimer, Macromolecules **22**, 1946 (1989).

[14] F. Schosseler, H. Benoit, Z. Grubisic-Gallot, Cl. Strazielle, and L. Leibler, Macromolecules **22**, 400 (1989).

[15] D. Durand, F. Naveau, and J. P. Busnel, Macromolecules **22**, 2011 (1989).
[16] M. Adam and M. Delsanti, Contemp. Phys. **30**, 203 (1989).
[17] J. E. Martin and J. Wilcoxon, Phys. Rev. A **39**, 252 (1989).
[18] F. Schosseler, M. Daoud, and L. Leibler, J. Phys. (France) **51**, 2373 (1990).
[19] J. E. Martin and J. Odinek, Macromolecules **23**, 3363 (1990).
[20] J. Bauer, P. Lang, W. Burchard, and M. Bauer, Macromolecules **24**, 2634 (1991).
[21] M. Adam, Makromol. Chem. Macromol. Symp. **45**, 1 (1991).
[22] J. R. Colby, M. Rubinstein, J. R. Gillmor, and T. H. Mourey, Macromolecules **25**, 7180 (1992).
[23] J. R. Colby, J. R. Gillmor, and M. Rubinstein, Phys. Rev. E **43**, 3712 (1993).
[24] P. Manneville and L. de Seze, in *Numerical Methods in the Study of Critical Phenomena*, edited by I. Della Dra, J. Demongeot, and B. Lacolle (Springer-Verlag, Berlin, 1981).
[25] H. J. Herrmann, D. P. Landau, and D. Stauffer, Phys. Rev. Lett. **49**, 412 (1982).
[26] R. Bansil, H. J. Herrmann, and D. Stauffer, J. Polym. Sci. **17**, 988 (1984); N. Jan, T. Lookman, and D. Stauffer, J. Phys. A **16**, L117 (1983); R. B. Pandey, J. Stat. Phys. **34**, 191 (1983).
[27] H. J. Herrmann, Phys. Rep. **136**, 153 (1986).
[28] C. N. Bowman and N. A. Peppas, Chem. Eng. Sci. **47**, 1411 (1992).
[29] H. Boots and R. B. Pandey, Polym. Bull. **11**, 415 (1984).
[30] Y. Y. Chiu and L. J. Lee, J. Polym. Sci. A **33**, 269 (1995).
[31] Y. Liu and R. B. Pandey, J. Phys. (France) II **4**, 865 (1994).
[32] Y. K. Leung and B. E. Eichinger, J. Chem. Phys. **80**, 3887 (1984).
[33] A. M. Gupta, R. C.Hendrickson, and C. W. Macosko, J. Chem. Phys. **95**, 2097 (1991).
[34] M. Rosche and M. Schulz, Makromol. Chem. Theory Simul. **2**, 361 (1993).
[35] P. Meakin, Phys. Rev. Lett. **51**, 1119 (1983).
[36] R. Julien and R. Bötet, *Aggregation and Fractal Aggregates* (World Scientific, Singapore, 1987).
[37] P. A. Netz and D. Samios, Macromol. Chem., Theory Simul. **3**, 607 (1994).
[38] R. M. Ziff, in *Kinetics of Aggregation and Gelation*, edited by F. Family and D. P. Landau (North-Holland, Amsterdam, 1984).
[39] M. H. Ernst, in *Fractals in Physics*, edited by L. Pietronero and E. Tosatti (Elsevier, New York, 1986).
[40] M. Klein, J-M. Guenet, A. Brulet, and F. Boue, Polymer **32**, 1943 (1991).
[41] E. M. de Oliveira Lima and F. Galembeck, J. Colloid. Interface Sci. **166**, 309 (1994).
[42] N. Fazel, A. Brulet, and J-M. Guenet, Macromolecules **27**, 3836 (1994).
[43] C. S. Kuo, R. Bansil, and C. Koňák, Macromolecules **28**, 768 (1995).
[44] S. Mal, P. Maiti, and A. K. Nandi, Macromolecules **28**, 237 (1995).
[45] K. A. Mauritz and R. M. Warren, Macromolecules **22**, 1730 (1989); K. A. Mauritz, I. D. Stefanithis, S. V. Davis, R. W. Scheetz, R. K. Pope, G. L. Wilkes, and H-H. Huang, J. Appl. Polym. Sci. **55**, 181 (1995); P. L. Shao, K. A. Mauritz, and R. B. Moore, Chem. Mater. **7**, 192 (1995).
[46] Y. Liu and R. B. Pandey, J. Chem. Phys. **105**, 825 (1996); Phys. Rev. E **54**, 6609 (1996).
[47] S. C. Glotzer, M. F. Gyure, F. Sciortino, A. Coniglio, and H.E. Stanley, Phys. Rev. Lett. **70**, 3275 (1993); Phys. Rev. E **49**, 247 (1994).